

Kondo-hole conduction in the La-doped Kondo insulator $\text{Ce}_3\text{Bi}_4\text{Pt}_3$

T. Pietrus,¹ H. v. Löhneysen,^{1,2} and P. Schlottmann³

¹Physikalisches Institut, Universität Karlsruhe, D-76128 Karlsruhe, Germany

²Forschungszentrum Karlsruhe, Institut für Festkörperphysik, D-76021 Karlsruhe, Germany

³Department of Physics, Florida State University, Tallahassee, Florida 32306, USA

(Received 20 September 2007; revised manuscript received 7 November 2007; published 25 March 2008)

The resistivity, Hall constant, specific heat, and magnetic susceptibility of the doped Kondo insulator $(\text{Ce}_{1-x}\text{La}_x)_3\text{Bi}_4\text{Pt}_3$ are studied as a function of temperature and x . Already at $x=0.006$, the alloy behaves like a metal, so that the metal-insulator transition in the impurity band must occur at a lower concentration. Our data allow to determine the effective mass m^* and the carrier concentration n separately. After a strong initial increase of $n(x)$, the carrier concentration remains nearly constant between $x=0.1$ and 0.5 . The effective mass in the metallic state initially increases with x and reaches a maximum of $m^* \approx 100m_0$ at $x=0.3$. The scattering time τ as determined from the Drude formula decreases drastically between $x=0.006$ and 0.1 , has a minimum at about $x=0.1$, and then a maximum at $x=0.3$. Surprisingly, m^*/τ is nearly constant for the entire alloy range for $x \geq 0.1$.

DOI: 10.1103/PhysRevB.77.115134

PACS number(s): 75.20.Hr, 75.30.Mb, 71.27.+a

I. INTRODUCTION

Kondo insulators are stoichiometric compounds with small-gap semiconducting properties.^{1,2} Most Kondo insulators do not show magnetic order, e.g., CeNiSn , $\text{Ce}_3\text{Bi}_4\text{Pt}_3$, YbB_{12} , FeSi , and SmB_6 (exceptions are the ferromagnet UF_4P_{12} and the antiferromagnet SmTe), with a Van-Vleck-like low-temperature susceptibility. The low- T resistivity and electronic specific heat approximately follow an exponential activation law¹ consistent with an energy gap in the density of states. Kondo insulators are not perfect semiconductors, because the gap is frequently only a pseudogap and/or there are intrinsic or impurity states in the band gap.

Within the framework of the periodic Anderson model, the energy gap in Kondo insulators arises from the hybridization between the $4f$ and conduction bands as a consequence of the coherence of the heavy-quasiparticle states at the Fermi level.² This indirect gap opens when the localized $4f$ level is close to the Fermi energy, and is most easily realized in crystals with cubic symmetry. The hybridization gap is strongly reduced by many-body interactions (Kondo effect) and can range from 1 to 50 meV. In contrast to usual band gaps, the gap of a Kondo insulator is strongly temperature dependent,^{3,4} and these materials become metallic above surprisingly low temperatures already. The gap can also be gradually closed by large magnetic fields, yielding a metallic state for fields larger than a critical one.⁵ This metal-insulator transition as a function of field has been observed in the specific heat of $\text{Ce}_3\text{Bi}_4\text{Pt}_3$ (Ref. 6) and in the magnetoresistance of YbB_{12} .⁷ The metal-insulator transition can also be induced by pressure and alloying. For instance, electrical conductivity and Hall-effect measurements on SmB_6 indicate that the gap jumps to zero discontinuously at 45 kbar,⁸ and for the alloy $\text{FeSi}_{1-x}\text{Ge}_x$, the gap in the resistivity decreases continuously with x and disappears at $x \approx 0.25$,⁹ with the system becoming metallic for $x > 0.25$. For Ce compounds, on the other hand, the hybridization is enhanced under pressure and the gap of $\text{Ce}_3\text{Bi}_4\text{Pt}_3$ increases.¹⁰

In this paper, we present low-temperature measurements of the conductivity, the Hall effect, the specific heat, and the

magnetic dc susceptibility for the La-doped Kondo insulator $\text{Ce}_3\text{Bi}_4\text{Pt}_3$ for various concentrations. Each La ion substituting a Ce ion represents a charge-neutral (both ions are nearly trivalent) perturbation that breaks the translational invariance of the lattice and introduces a bound state in the narrow gap of the semiconductor.¹¹⁻¹³ With increasing concentration, the bound states at different sites overlap and eventually form an impurity band that pins the Fermi level. For very small La concentrations, the states of the impurity band are expected to be localized due to the disorder and a metal-insulator transition is induced when the states at the Fermi level acquire a finite mobility.

Our main results are the following. The metal-insulator transition already occurs at a concentration less than $x = 0.006$. Hence, a metallic state is realized for very low x in the impurity band. Using Fermi-liquid arguments, our data allow us to determine the effective mass m^* and the carrier concentration n separately. The effective mass in the metallic state initially increases with x and reaches a maximum of $m^* \approx 100m_0$ at $x=0.3$, where m_0 is the free electron mass. The carrier concentration, after a strong initial increase, remains nearly constant between $x=0.1$ and 0.5 . We further find that $\sigma \sim x^{1/3}$. Combining these results with the Drude model, the scattering time τ is found to decrease by more than a factor of 2 between $x=0.006$ and 0.1 , has a minimum at about $x=0.1$, and then passes over a maximum at $x=0.3$. Surprisingly, m^*/τ is nearly constant over the entire alloy range for $x \geq 0.1$.

The paper is organized as follows. In Sec. II, we briefly summarize the crystal growth and measurement methods. In Sec. III, we discuss the known properties of the stoichiometric compound $\text{Ce}_3\text{Bi}_4\text{Pt}_3$, in particular, the existence of intrinsic vs extrinsic in-gap bound states. In Sec. IV, we present our results for the $(\text{Ce}_{1-x}\text{La}_x)_3\text{Bi}_4\text{Pt}_3$ alloys with special emphasis on the properties of the impurity band, and compare them with previous studies. Concluding remarks follow in Sec. V.

II. EXPERIMENT

$(\text{Ce}_{1-x}\text{La}_x)_3\text{Bi}_4\text{Pt}_3$ single crystals were grown in a Bi flux from Ce 4 mN, La 3 mN, Pt 5 mN, and Bi 6 mN in an Al_2O_3 crucible sealed under 10^{-6} mbar in a quartz tube. The tube was heated to 1150 °C and, after 12 h, was cooled very slowly to 850 °C at a rate of -1 K/h. After cooling to 450 K, the crucible was centrifuged to separate excess Bi flux. The resultant small single crystals (typically $1 \times 0.2 \times 0.2$ mm³) were checked under an optical microscope for Bi residues, which were then removed mechanically if present. The lattice constants (crystal structure: cubic $I43d$) of the alloys were determined as $a = (10.45 \pm 0.081x)$ Å.

For four-probe resistivity and Hall-effect measurements, 50- μm -thick Au leads were attached to the sample with conducting paste. Because of the large error in the geometry owing to the small sample size, only resistance ratios ρ/ρ_{300} with respect to the room-temperature value ρ_{300} will be shown. For our analysis below, we use $\rho_{300}(x) = (220 - 70x)$ $\mu\Omega$ cm. The Hall coefficient R_H was determined in $B = 5$ T with positive and negative field polarities to eliminate contributions of the longitudinal voltage drop due to misalignment of the Hall contacts.

The specific heat was measured with the semiadiabatic heat-pulse technique, with the sample attached with Apiezon W grease to a sapphire plate whose opposite side carried an evaporated heater and a carbon resistance thermometer.¹⁴ The linear specific-heat coefficient γ was determined from a least-squares fit of $C/T = \gamma T + \beta T^3$ to the data between 1.5 and 5 K. The magnetic dc susceptibility of single-crystalline $\text{Ce}_3\text{Bi}_4\text{Pt}_3$ was measured in a superconducting quantum interference device magnetometer in a magnetic field of 0.1 T. For the $(\text{Ce}_{1-x}\text{La}_x)_3\text{Bi}_4\text{Pt}_3$, several small pieces were measured together in a field of 1 mT.

III. IN-GAP BOUND STATES IN THE STOICHIOMETRIC COMPOUND $\text{Ce}_3\text{Bi}_4\text{Pt}_3$

Numerous properties of the Kondo insulator $\text{Ce}_3\text{Bi}_4\text{Pt}_3$ have been thoroughly studied. The Ce ions have a small valence admixture from the tetravalent configuration, so that $n_f \approx 0.9$.¹⁵ Below 50 K, the electrical resistivity rises sharply and the overall behavior is roughly described by a temperature-dependent activation energy $\Delta \sim 35$ –60 K,^{16–19} corresponding to a small indirect gap E_g of about 120 K for $T \rightarrow 0$ (in transport measurements, the activation energy is $E_g/2$). This behavior arises from the promotion of electrons from the top of the valence band to the bottom of the conduction band. As expected, a much larger gap of ~ 300 cm⁻¹, corresponding to the direct gap between the valence and conduction bands, is measured by infrared reflectivity.²⁰ A spin gap corresponding in magnitude to E_g has been observed by inelastic neutron scattering.^{21,22} The magnetic susceptibility displays the typical Curie-Weiss behavior at high temperatures, has a maximum at $T \approx E_g$, and then decreases with decreasing temperature. At the lowest T , the susceptibility has a sharp upturn, which is very sensitive to a magnetic field and is frequently attributed to impurities. Except for this upturn, the inelastic neutron-scattering results reproduce the temperature dependence of the susceptibility.²¹

Similar to other Kondo insulators, such as FeSi (Ref. 23) and SmB_6 ,²⁴ the properties of $\text{Ce}_3\text{Bi}_4\text{Pt}_3$ can be classified using several temperature ranges. (i) Above 80 K, the magnetic susceptibility is Curie-Weiss-like,¹⁶ the electrical conductivity is almost temperature independent,¹⁶ the gap is smeared by temperature,²⁰ and the material behaves like a poor metal. (ii) For $80 \text{ K} > T > 10 \text{ K}$, when T is lowered, the conductivity decreases exponentially and the susceptibility decreases slightly.¹⁶ (iii) Below 10 K, the resistivity saturates,¹⁰ the susceptibility has an upturn,¹⁶ and the specific heat follows a metallic behavior,^{6,16} i.e., $C = \gamma T + \beta T^3$, although we are dealing with a narrow-gap semiconductor. This temperature range is believed to be dominated by in-gap states.

Evidence for in-gap states has also been found for FeSi,^{3,23} YbB_{12} ,²⁵ and SmB_6 .^{24,26–28} These in-gap states are believed to be a common feature to all Kondo insulators.²⁹ In-gap states can be intrinsic to the material or extrinsic arising from defects, i.e., vacancies on Ce sites or a deficiency on ligand sites. The nature of the in-gap bound states, whether intrinsic or extrinsic, is still controversial. The in-gap states are sample dependent, but their effects (e.g., on the specific-heat coefficient γ) are large, so that it is difficult to associate them with lattice defects. It is very likely that the in-gap states are an intrinsic property of Kondo insulators.

Several models have been proposed for intrinsic in-gap states. Within the framework of a localized model, Kasuya³⁰ predicted two different temperature regimes in SmB_6 . The lowest excitation state is an s -wave exciton, leading to predictions consistent with the neutron-scattering results. Along somewhat similar lines, Riseborough^{29,31} proposed that the intermediate-valence nature of the system gives rise to antiferromagnetic correlations leading to in-gap magnetic excitations, analogous to paramagnons arising from antiferromagnetic (rather than ferromagnetic) correlations in a metal. These excitonlike states depend strongly on temperature and magnetic field.²⁴ It has been suggested^{29,31} that Kondo insulators are close to an antiferromagnetic phase transition at low temperatures. This has been verified in a few cases, e.g., in CeNiSn , where Cu doping introduces magnetic order.³² Antiferromagnetism in Kondo insulators with bipartite lattices had previously been predicted.³³

Our data for the stoichiometric compound—some of which will be shown below in conjunction with those of the alloy series—are in agreement with the published results. Note that the physics of the excitonlike intrinsic in-gap bound states discussed above is very different from the impurity-band bound states addressed in Sec. IV.

IV. IMPURITY BAND IN $(\text{Ce}_{1-x}\text{La}_x)_3\text{Bi}_4\text{Pt}_3$ ALLOYS

Figure 1 shows the resistivity ρ as a function of temperature T , normalized to its room-temperature value ρ_{300} , for various $(\text{Ce}_{1-x}\text{La}_x)_3\text{Bi}_4\text{Pt}_3$ samples with $0 \leq x \leq 1$. The strong increase of ρ for $x=0$ at low T as the temperature is reduced is an indication of the good quality of the samples. Already for $x=0.006$, ρ/ρ_{300} has decreased by nearly 2 orders of magnitude. For $x=0.006$ and 0.1, maxima in $\rho(T)$ are seen at low T . For $x=0.5$, ρ is nearly independent of T , while for

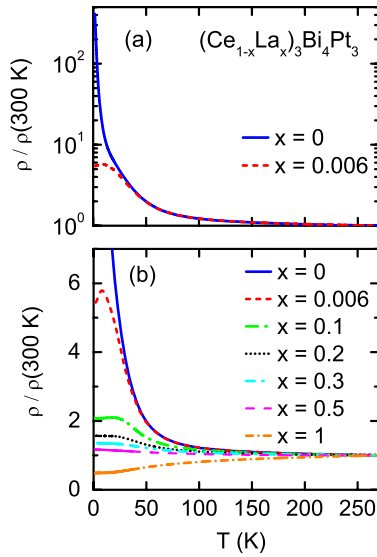


FIG. 1. (Color online) The resistivity ρ for $(\text{Ce}_{1-x}\text{La}_x)_3\text{Bi}_4\text{Pt}_3$ as a function of T normalized to its value at room-temperature ρ_{300} for various La concentrations. Note that in the upper panel, the scale of ρ is logarithmic, while in the lower panel, this scale is linear.

$x=1$, metallic behavior, i.e., $d\rho/dT > 0$, is observed in the whole T range investigated.

Figure 2 shows $\ln(\rho/\rho_{300})$ plotted against T^{-1} for various x . Over the limited temperature range $70 \text{ K} \leq T \leq 100 \text{ K}$, $\rho(T)$ can be described by a simple Arrhenius law up to $x=0.5$, where the activation energies are $E_g/k_B=92, 92, 54, 31, 24$, and 6 K for $x=0, 0.006, 0.1, 0.2, 0.3$, and 0.5 , respectively. The activation energy depends on the temperature range considered, i.e., E_g decreases with increasing T , as can be inferred from the upward curvature for low- x samples, as has been found before for $\text{Ce}_3\text{Bi}_4\text{Pt}_3$.¹⁸ It also should be pointed out that for the T range chosen for our fits, the criterion $k_B T \ll E_g$ is not satisfied. Our data are in good agreement with previously published results.^{18,19,34}

The T dependence of the carrier concentration $n = 1/|eR_H|$ for different samples is displayed in Fig. 3. We have observed a negative sign of the Hall coefficient R_H ,

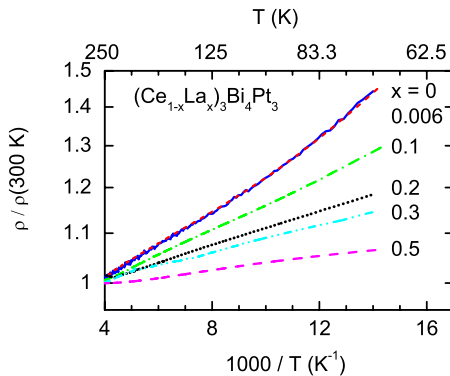


FIG. 2. (Color online) Logarithm of the normalized resistivity $\rho/\rho(300 \text{ K})$ as a function of T^{-1} for various La concentrations x . The slopes of the curves correspond to the activation energy. The corresponding values of T are indicated on the upper horizontal axis.

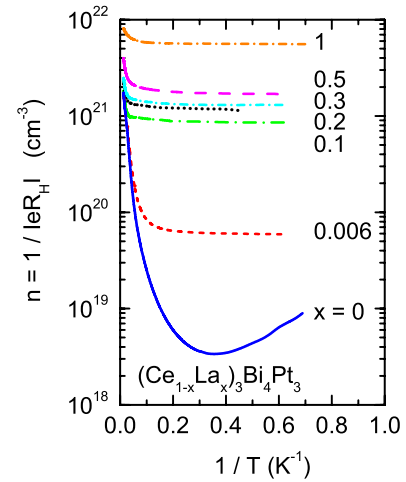


FIG. 3. (Color online) Carrier density n plotted logarithmically as a function of T^{-1} , determined from the Hall constant measured in a magnetic field of 5 T for several La concentrations x . The corresponding values of T are indicated on the upper horizontal axis.

showing that the carriers are electronlike.³⁵ Here, we assume that only one band contributes to charge transport. For $T > 40 \text{ K}$, the carrier density clearly increases with T for all concentrations. This is the temperature range where the gap is already closing for pure $\text{Ce}_3\text{Bi}_4\text{Pt}_3$, as observed via infrared spectroscopy.²⁰ The behavior is then metallic and qualitatively similar to that of $\text{La}_3\text{Bi}_4\text{Pt}_3$. The $n(T)$ curve for $x=0$ is qualitatively different from those for $x \geq 0.006$ at lower $T \leq 10 \text{ K}$: For $x \geq 0.006$, the number of carriers is constant with T in this temperature range, while for $x=0$, a pronounced minimum of $n(T)$ is observed at $T=2.9 \text{ K}$. The carrier density increases systematically with x . The independence of T already for $x=0.006$ indicates that the metallic character prevails down to very low La concentrations.

The finite carrier concentration of the doped Kondo semiconductor is the consequence of the impurity band that develops in the gap. Each La impurity breaks the translational invariance of the lattice and gives rise to a bound state in the gap. The substitution is nearly charge neutral, since both ions, Ce and La, are believed to be close to being trivalent. The only difference is that in the case of La, the $4f$ orbital is not occupied. This can be modeled with a very large repulsive potential for the $4f$ states at the La site.³⁶ For very low x , the bound states are isolated and localized. With increasing x , they start to overlap and develop into an impurity band. The corresponding density of states has a height and width approximately proportional to $x^{1/2}$. The number of states contained in the impurity band is Nx , where N is the number of rare-earth sites. The Fermi level is expected to be roughly at the center of the density of states of the impurity band.¹¹ For very low x , the states are localized and eventually become conducting in the neighborhood of the Fermi level with increasing x . For $(\text{Ce}_{1-x}\text{La}_x)_3\text{Bi}_4\text{Pt}_3$, this metal-insulator transition occurs at a doping level x smaller than 0.006 .

The analysis of the nonmonotonic $n(T)$ dependence for the stoichiometric compound $\text{Ce}_3\text{Bi}_4\text{Pt}_3$ can also be inferred from previous R_H measurements.¹⁷ It cannot be explained by a simple one-band model of free carriers. Note that at T

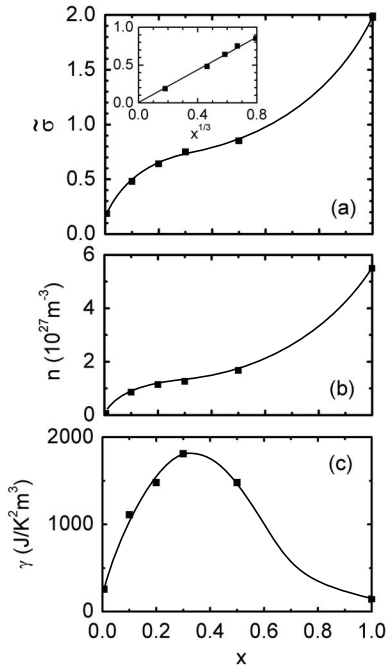


FIG. 4. Comparison of properties of $(\text{Ce}_{1-x}\text{La}_x)\text{Bi}_4\text{Pt}_3$: (a) Conductivity $\tilde{\sigma}$ at 2.5 K normalized to the conductivity at room temperature, (b) carrier concentration n extrapolated to $T \rightarrow 0$ (from Fig. 3), and (c) linear specific-heat coefficient γ , as a function of the La concentration x . In order to facilitate the direct comparison with n , γ is given in units of $\text{J/K}^2 \text{ m}^3$. For $\text{Ce}_3\text{Bi}_4\text{Pt}_3$ ($x=0$), $1000 \text{ J/K}^2 \text{ m}^3$ correspond to $0.459 \text{ J/K}^2 \text{ mol}$ $\text{Ce}_3\text{Bi}_4\text{Pt}_3$. The solid curves are a guide for the eye. Inset in (a) shows $\tilde{\sigma}$ vs $x^{1/3}$ for $x \leq 0.3$.

$=3 \text{ K}$, the number of carriers for $x=0$ is smaller than for $x=0.006$ by more than 1 order of magnitude. The origin of the carriers is not the La Kondo-hole impurity band, but rather the in-gap states discussed in Sec. III: The in-gap states can be extrinsic (e.g., Ce vacancies, Bi or Pt vacancies, or interchanged lattice sites) or intrinsic (many-body collective modes²⁹) to the material. The substantial “metallic” specific-heat coefficient γ suggests that the density of states at the Fermi level is larger than that corresponding to 10^{25} free-electron-like carriers per m^3 . These states are then either localized due to disorder or might be arising from the magnetic exciton bound states suggested by Riseborough.^{29,31} The strong magnetic-field dependence of the in-gap states found for other Kondo insulators (see, e.g., Ref. 24) is an indication that the states are not simple impurity bound states. This is also a plausible explanation for the low- T upturn of the magnetic susceptibility of $\text{Ce}_3\text{Bi}_4\text{Pt}_3$ and other Kondo insulators. The exciton bound states have a finite lifetime due to residual interactions and it is not known how they contribute to the conductivity and the specific-heat coefficient γ .

We now focus on the low- T conductivity data of the Kondo-hole impurity band, i.e., on the data for $0.006 \leq x \leq 0.5$. Figure 4 compares the concentration dependence of $\tilde{\sigma} = \sigma(2.5 \text{ K}) / \sigma_{300}$, n in the plateau region for $T \rightarrow 0$ (cf. Fig. 3), and the linear specific-heat coefficient γ . The carrier concentration increases from $0.6 \times 10^{26} \text{ m}^{-3}$ for $x=0.006$ to $0.86 \times 10^{27} \text{ m}^{-3}$ for $x=0.1$. Beyond $x=0.1$, n increases only

gradually up to $x=0.5$, reaching $1.67 \times 10^{27} \text{ m}^{-3}$, and then rises to $5.5 \times 10^{27} \text{ m}^{-3}$ for $x=1$. The fact that n does not grow linearly with x for small x indicates that not all the impurity states are mobile. The linear specific-heat coefficient, on the other hand, measures the total density of states (whether localized or delocalized) at the Fermi level. γ increases with x from the modest value at $x=0$ discussed in Sec. III above, goes through a maximum at $x=0.3$, and then gradually decreases. Our data for $\gamma(x)$ agree very well with previous measurements by Canfield *et al.*³⁴ For small x , we expect that $\gamma \propto \sqrt{x}$; while for large x , the Ce sites are sparse and, consequently, the correlations in the $4f$ shell and the hybridization fade away. In the limit $x \rightarrow 1$, the system is metallic and the Ce ions can be considered as Kondo impurities and γ should be approximately linear in $1-x$, the concentration of Ce ions. Consequently, $\gamma(x)$ should pass over a maximum which is, indeed, observed.

The x dependence of the conductivity at 2.5 K, shown in Fig. 4, is approximately proportional to $x^{1/3}$ for small x [see inset of Fig. 4(a)]. In a nearly-free-electron picture, the conductivity is given by the product of the mobility and the density in each carrier band. We assume here that the Kondo holes contribute to only one electronlike band. The comparison of Figs. 4(a) and 4(b) shows that $\tilde{\sigma}(x)$ and $n(x)$ exhibit an overall similar behavior, implying that the mobility is roughly independent of x for $0.1 \leq x \leq 0.5$. However, one notes that for $x=0.006$, $\tilde{\sigma}$ has already acquired a sizable value while n is still less than 10% of the value for $x=0.1$. This contrasts the concept of a mobility edge, where states with energy less than the mobility edge are localized and those above are conducting.

Assuming that there is a metal-insulator transition at $x_c < 0.006$, for $T \rightarrow 0$ we may write $\tilde{\sigma} \sim (x-x_c)^p$, where p is the critical conductivity exponent. While with the present data we are unable to determine x_c accurately, the upper bound $x_c < 0.006$ implies that $p \approx 1/3$ [inset of Fig. 4(a)]. We note that $p=1/3$ is much smaller than the lower limit for a metal-insulator transition when identifying the exponent p with the correlation-length exponent ν , for which $\nu > 2/3$ is predicted.³⁷ This might indicate that the Kondo-hole-induced transition is a special case. Theoretical attempts to calculate x_c are limited to bands with nearest-neighbor tight-binding hopping and the electron-hole symmetric situation.³⁸ The critical concentration is expected to decrease with increasing hopping range and electron-hole asymmetry.

In the following, we will interpret our low-temperature data within a single-band Drude model. For the impurity band, we assume a parabolic dispersion with spherical Fermi surface and effective mass m^* . This, of course, imposes strong limitations on the interpretation, which, however, is appealing because of its simplicity. From $n(x)$, we can determine the Fermi wave vector $k_F = (3\pi^2 n)^{1/3}$. The electronic specific-heat coefficient is then $\gamma = (k_B^2 / 3\hbar^2) m^* k_F$. Using k_F and the measured γ , we obtain the effective mass m^* , which is shown as a function of x in Fig. 5(a). m^* reaches a maximum of $105m_0$ for $x=0.3$ and decreases to $5m_0$ for $\text{La}_3\text{Bi}_4\text{Pt}_3$. This demonstrates the heavy-quasiparticle character of the excitations in the impurity band, contrasting the behavior of conventional doped semiconductors such as Si:P.^{39,40} Note that m^* is largest when the hybridization gap

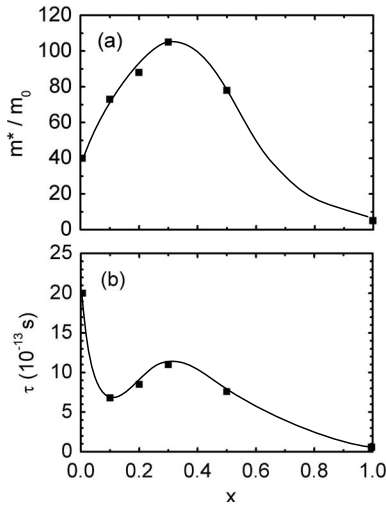


FIG. 5. (a) Effective mass of the quasiparticles in the Kondo-hole impurity band in units of the free electron mass and (b) the Drude scattering time τ at low T as a function of the La concentration x . See the text for the definition of these quantities. The solid curves are a guide for the eye.

is closing, as can be seen by comparison with the lower panel of Fig. 1. A more detailed analysis requires taking into account the simultaneous destruction of the hybridization gap due to incoherent scattering in the alloy and the formation of the impurity band as a function of x .

In Fig. 5(b), we show the Drude scattering time $\tau = \sigma m^*/ne^2$ derived using the measured σ and n , and the calculated m^* from Fig. 5(a). As expected, τ is very large for small x (there are only a few scattering centers), then it decreases rapidly with x , and undergoes a minimum around $x = 0.1$ and, subsequently, a maximum with $\tau \approx 1.1 \times 10^{-12}$ at $x \approx 0.3$. For larger x , it decreases down to $\tau \approx 4.4 \times 10^{-14}$ for $\text{La}_3\text{Bi}_4\text{Pt}_3$.

Finally, the dc susceptibility defined as $\chi_{dc} = M/B$ is presented in Fig. 6. The data for $\text{Ce}_3\text{Bi}_4\text{Pt}_3$ shown in Fig. 6(a) are in good qualitative agreement with previously published results.¹⁶ In both cases, the samples are single crystals. The upturn at low T is less pronounced for the present sample, and the ratio of the maximum to the minimum value is also larger than for the crystal in Ref. 16. The minimum at low T arises from the spin gap associated with the hybridization gap, and the maximum is the consequence of electronic transitions from the valence band into the conduction band and is consistent with an indirect gap of about 70 K. At high $T > 100$ K, a Curie-Weiss-like behavior is observed. The Weiss temperature is approximately -100 K, i.e., consistent with the gap. The origin of the small upturn at low T are the in-gap states discussed above, which are common to all Kondo insulators. The low- T susceptibility remains substantial, probably as a consequence of Van Vleck terms.

In Fig. 6(b), the T dependence of χ_{dc} is displayed for polycrystalline samples with several concentrations x . The minimum of χ_{dc} at low T is gradually smeared with the La-impurity concentration. The gap becomes less well defined with increasing x and, consequently, the height of the maximum rapidly decreases. The temperature of the maximum

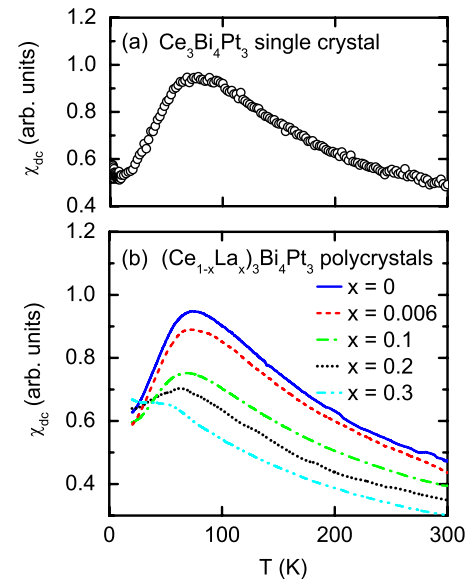


FIG. 6. (Color online) The magnetic dc susceptibility, $\chi_{dc} = M/B$, of $(\text{Ce}_{1-x}\text{La}_x)_3\text{Bi}_4\text{Pt}_3$ as a function of temperature for several La concentrations x . The data in (a) were obtained for single crystal with $x=0$, while those in (b) were obtained for polycrystalline samples for various x .

also decreases with x , which is a sign that the gap is reduced. For $T > 100$ K, the susceptibility is still Curie-Weiss-like, but with Weiss temperature increasing with x .

V. CONCLUDING REMARKS

We have studied the La-doped Kondo insulator $\text{Ce}_3\text{Bi}_4\text{Pt}_3$. The substitution of Ce by La introduces Kondo-hole bound states, which, with increasing x , eventually form an impurity band. These Kondo-hole bound states are very different from the in-gap states of the stoichiometric semiconductor $\text{Ce}_3\text{Bi}_4\text{Pt}_3$. According to Kasuya³⁰ and Riseborough,³¹ the states for the pure undoped semiconductor are excitonlike collective many-body excitations intrinsically present in all Kondo insulators. Although their intrinsic character is highly plausible because of the high quality of many samples, their nature has not yet been determined. An impurity band in doped Kondo insulators (e.g., La substituting for Ce) is qualitatively different from more classical semiconductor systems exhibiting a metal-insulator transition as a function of doping, e.g., Si:P (Refs. 41–43) or Si:B,⁴⁴ where disorder and concomitant electron-electron interactions lead to electron localization. Nevertheless, when doped deep into the metallic region, both types of systems exhibit nearly-free-electron behavior.

There are two main differences distinguishing impurity bands in classical semiconductors from Kondo insulators. (1) The gap in Kondo insulators is a hybridization gap, which is small due to the strong correlations, and not a band gap as in Si or Ge. These correlations lead to a strong decrease of the Kondo-insulator gap with increasing temperature, which closes at already quite low T . Furthermore, the gap is gradually suppressed with increasing concentration of Kondo

holes. (2) Doping in classical semiconductors provides carriers which for low concentrations are localized in hydrogenic bound states and eventually give rise to an impurity band with increasing concentration. In particular, for shallow donors or acceptors, e.g., for Si:P or Si:B, the large spatial extent of the dopant wave function leads to a metal-insulator transition within the impurity band at very low doping levels. Hence, the electronic structure of the valence and conduction bands and, notably, the energy gap remain essentially unaltered by doping. The substitution of Ce by La, on the other hand, is charge neutral (neglecting the small $4f$ admixture) and the bound states are split-off states from the valence and conduction bands, rather than hydrogenic bound states. Furthermore, the Kondo holes generate an impurity band, which gradually closes the hybridization gap.

The focus of this study has been on the region of doping where $(\text{Ce}_{1-x}\text{La}_x)_3\text{Bi}_4\text{Pt}_3$ is already metallic, i.e., for $x \geq 0.006$. Assuming a Fermi-liquid-like behavior for quasi-free-electrons (parabolic dispersion), the data allow us to determine separately the effective mass m^* and the carrier concentration n from the Hall constant and the specific-heat coefficient γ . While the effective mass increases with x for small concentrations, reaches a maximum of $m^* \approx 100m_0$ at $x=0.3$, and decreases monotonically to $5m_0$ for $\text{La}_3\text{Bi}_4\text{Pt}_3$, the carrier density remains essentially constant between $x=0.1$ and 0.5 after a strong initial increase for small x . Sur-

prisingly, we find that at low T , $\sigma \sim x^{1/3}$. However, the La concentration range of our samples is too sparse for small x to attempt to determine x_c , the critical concentration of the metal-insulator transition.

Combining these results with the Drude model, the scattering time τ is found to decrease initially by more than a factor of 2 between $x=0.006$ and 0.1 , then it has a minimum at about $x=0.1$, passes over a maximum at approximately $x=0.3$, and finally decreases to a short $\tau \approx 4.4 \times 10^{-14}$ s for $x=1$. Surprisingly, m^*/τ is nearly constant for $x \geq 0.1$ for the entire alloy range. This value is much smaller for $x=0.006$, which is a sign that one is approaching the insulating regime.

ACKNOWLEDGMENTS

We thank J. Hagel and M. Kelemen for performing the susceptibility measurements, and G. Müller-Vogt and M. Steinbach for their help in sample preparation. T.P. acknowledges the hospitality of T. Takabatake at Hiroshima University, where he was introduced to the flux-growth technique. The support by the Deutsche Forschungsgemeinschaft under the auspices of SFB 195, the Helmholtz Association of German Research Centers under Grant No. VIRQ-VH-VI-127, and the U.S. Department of Energy under Grant No. DE-FG02-98ER45707 is acknowledged.

-
- ¹G. Aeppli and Z. Fisk, *Comments Condens. Matter Phys.* **16**, 155 (1992).
- ²P. Riseborough, *Adv. Phys.* **49**, 257 (2000).
- ³Z. Schlesinger, Z. Fisk, H. T. Zhang, M. B. Maple, J. F. DiTusa, and G. Aeppli, *Phys. Rev. Lett.* **71**, 1748 (1993).
- ⁴L. Degiorgi, *Rev. Mod. Phys.* **71**, 687 (1999).
- ⁵A. J. Millis, in *Physical Phenomena at High Magnetic Fields*, edited by E. Manousaki, P. Schlottmann, and P. Kumar (Addison-Wesley, Reading, MA, 1991), p. 146.
- ⁶M. Jaime, R. Movshovich, G. R. Stewart, W. P. Beyermann, M. G. Berisso, M. F. Hundley, P. C. Canfield, and J. L. Sarrao, *Nature (London)* **405**, 160 (2000).
- ⁷K. Sugiyama, F. Iga, M. Kasaya, T. Kasuya, and M. Date, *J. Phys. Soc. Jpn.* **57**, 3946 (1988).
- ⁸J. C. Cooley, M. C. Aronson, Z. Fisk, and P. C. Canfield, *Phys. Rev. Lett.* **74**, 1629 (1995); J. C. Cooley, M. C. Aronson, A. Lacerda, Z. Fisk, P. C. Canfield, and R. P. Guertin, *Phys. Rev. B* **52**, 7322 (1995).
- ⁹S. Yeo, S. Nakatsui, A. D. Bianchi, P. Schlottmann, Z. Fisk, L. Balicas, P. A. Stampe, and R. J. Kennedy, *Phys. Rev. Lett.* **91**, 046401 (2003).
- ¹⁰J. C. Cooley, M. C. Aronson, and P. C. Canfield, *Phys. Rev. B* **55**, 7533 (1997).
- ¹¹P. Schlottmann, *Phys. Rev. B* **46**, 998 (1992); **54**, 12324 (1996).
- ¹²P. Schlottmann, *Physica B* **186-188**, 375 (1993).
- ¹³Z.-Z. Li, W. Xu, C. Chen, and M.-W. Xiao, *Phys. Rev. B* **50**, 11332 (1994).
- ¹⁴K. Albert, W. Sander, H. v. Löhneysen, and H. J. Schink, *Cryogenics* **22**, 417 (1982).
- ¹⁵G. H. Kwei, J. M. Lawrence, and P. C. Canfield, *Phys. Rev. B* **49**, 14708 (1994).
- ¹⁶M. F. Hundley, P. C. Canfield, J. D. Thompson, Z. Fisk, and J. M. Lawrence, *Phys. Rev. B* **42**, 6842 (1990).
- ¹⁷M. F. Hundley, P. C. Canfield, J. D. Thompson, Z. Fisk, and J. M. Lawrence, *Physica B* **171**, 254 (1991).
- ¹⁸M. F. Hundley, J. D. Thompson, P. C. Canfield, and Z. Fisk, *Physica B* **199-200**, 443 (1994).
- ¹⁹M. F. Hundley, P. C. Canfield, J. D. Thompson, and Z. Fisk, *Phys. Rev. B* **50**, 18142 (1994).
- ²⁰B. Bucher, Z. Schlesinger, P. C. Canfield, and Z. Fisk, *Phys. Rev. Lett.* **72**, 522 (1994).
- ²¹A. Severing, J. D. Thompson, P. C. Canfield, Z. Fisk, and P. Riseborough, *Phys. Rev. B* **44**, 6832 (1991).
- ²²P. S. Riseborough, *Phys. Rev. B* **45**, 13984 (1992).
- ²³N. E. Sluchanko, V. V. Glushkov, S. V. Demishev, A. A. Menovsky, L. Weckhuysen, and V. V. Moshchalkov, *Phys. Rev. B* **65**, 064404 (2002).
- ²⁴T. Caldwell, A. P. Reyes, W. G. Moulton, P. L. Kuhns, M. J. R. Hoch, P. Schlottmann, and Z. Fisk, *Phys. Rev. B* **75**, 075106 (2007).
- ²⁵A. Bouvet, T. Kasuya, M. Bonnet, L. P. Regnault, J. Rossat-Mignod, F. Iga, B. Fåk, and A. Severing, *J. Phys.: Condens. Matter* **10**, 5667 (1998).
- ²⁶T. Nanba, H. Ohta, M. Motokawa, S. Kimura, S. Kunii, and T. Kasuya, *Physica B* **186-188**, 440 (1993).
- ²⁷B. Gorshunov, N. Sluchanko, A. Volkov, M. Dressel, G. Knebel, A. Loidl, and S. Kunii, *Phys. Rev. B* **59**, 1808 (1999).
- ²⁸P. Nyhus, S. L. Cooper, Z. Fisk, and J. Sarrao, *Phys. Rev. B* **55**,

- 12488 (1997).
- ²⁹P. S. Riseborough, Phys. Rev. B **68**, 235213 (2003).
- ³⁰T. Kasuya, J. Phys. Soc. Jpn. **65**, 2548 (1996).
- ³¹P. Riseborough, Ann. Phys. **9**, 813 (2000).
- ³²T. Takabatake *et al.*, J. Magn. Magn. Mater. **177-181**, 277 (1998).
- ³³V. Dorin and P. Schlottmann, Phys. Rev. B **46**, 10800 (1992).
- ³⁴P. C. Canfield, J. D. Thompson, Z. Fisk, M. F. Hundley, and A. J. Lacerda, J. Magn. Magn. Mater. **108**, 217 (1992).
- ³⁵T. Pietrus, H. v. Löhneysen, B. Steinbach, and G. Müller-Vogt, Physica B **282-282**, 262 (2000).
- ³⁶R. Sollie and P. Schlottmann, J. Appl. Phys. **69**, 5478 (1991).
- ³⁷J. T. Chayes, L. Chayes, D. S. Fisher, and T. Spencer, Phys. Rev. Lett. **57**, 2999 (1986).
- ³⁸P. Schlottmann and C. S. Hellberg, J. Appl. Phys. **79**, 6414 (1996).
- ³⁹N. Kobayashi, S. Ikehata, S. Kobayashi, and W. Sasaki, Solid State Commun. **24**, 67 (1977); **32**, 1147 (1979).
- ⁴⁰M. Lakner and H. v. Löhneysen, Phys. Rev. Lett. **70**, 3475 (1993); M. Lakner, H. v. Löhneysen, A. Langenfeld, and P. Wölfle, Phys. Rev. B **50**, 17064 (1994).
- ⁴¹T. F. Rosenbaum, R. F. Milligan, M. A. Paalanen, G. A. Thomas, R. N. Bhatt, and W. Lin, Phys. Rev. B **27**, 7509 (1983).
- ⁴²X. Liu, A. Sidorenko, S. Wagner, P. Ziegler, and H. v. Löhneysen, Phys. Rev. Lett. **77**, 3395 (1996).
- ⁴³S. Waffenschmidt, C. Pfeleiderer, and H. v. Löhneysen, Phys. Rev. Lett. **83**, 3005 (1999).
- ⁴⁴M. P. Sarachik, A. Roy, and R. N. Bhatt, Solid State Commun. **60**, 513 (1986).